

DEFINITIVE COPY

STC TECHNOLOGY LTD

0377H

LONDON ROAD  
HARLOW  
ESSEX CM17 9NA  
TELEPHONE 0279 29531  
INTERNATIONAL + 44 279 29531  
TELEX 81151 STL HW G  
FAX 0279 441551

1

AD-A220 737

DTIC  
ELECTE  
APR 20 1990  
S D  
co

STL Technical Report  
IR/503/1990/1488

Contract No. N 00014-87-J-1258  
August 1987 - December 1989

NOVEL PULSED PLASMA TREATMENT  
& COATING PROCESS:  
MULTILAYER STRUCTURES FOR  
OPTICAL COMPUTING APPLICATIONS

Final Report

**DISTRIBUTION STATEMENT A**  
Approved for public release  
Distribution Unlimited

Prepared by : I. P. Llewellyn  
R. A. Heinecke  
Approved by : P. W. Graves  
Issued : March 1990

17 054

REGISTERED IN ENGLAND NO 401392  
REGISTERED OFFICE AND ADDRESS FOR SERVICE  
18 PORTLAND PLACE LONDON W1N 3AA  
A MANAGEMENT COMPANY OF STC PLC

**STRATEGIC DEFENSE INITIATIVE ORGANISATION  
INNOVATIVE SCIENCE & TECHNOLOGY OFFICE**

**Program Administered by  
OFFICE OF NAVAL RESEARCH**

**Contract N00014-87-J-1258**

**TECHNICAL REPORT NO. IR/503/1990/1488**

**NOVEL PULSED PLASMA TREATMENT & COATING PROCESS:  
MULTILAYER STRUCTURES FOR OPTICAL COMPUTING APPLICATIONS**

**by**

**I. P. Llewellyn and R. A. Heinecke**

**FINAL REPORT**

**STC Technology Ltd,  
Optoelectronics, Materials & Components Division  
London Road,  
Harlow, CM17 9NA, England**

**16th March 1990**

**Reproduction in whole or in part is permitted for any purpose  
of the United States Government**

**This document has been approved for public release and sale:  
its distribution is unlimited**

SECURITY CLASSIFICATION OF THIS PAGE

## REPORT DOCUMENTATION PAGE

1a. REPORT SECURITY CLASSIFICATION <b>Unclassified/Unlimited</b>		1b. RESTRICTIVE MARKINGS <b>None</b>	
2a. SECURITY CLASSIFICATION AUTHORITY		3. DISTRIBUTION/AVAILABILITY OF REPORT <b>Unrestricted</b>	
2b. DECLASSIFICATION/DOWNGRADING SCHEDULE			
4. PERFORMING ORGANIZATION REPORT NUMBER(S) <b>IR/503/1990/1488</b>		5. MONITORING ORGANIZATION REPORT NUMBER(S)	
6a. NAME OF PERFORMING ORGANIZATION <b>STC Technology Ltd</b>	6b. OFFICE SYMBOL (If applicable) <b>STL</b>	7a. NAME OF MONITORING ORGANIZATION <b>Office of Naval Research Dr. R. Pohanka</b>	
6c. ADDRESS (City, State, and ZIP Code) <b>London Road Harlow, Essex, CM17 9NA. England</b>		7b. ADDRESS (City, State, and ZIP Code) <b>Department of the Navy 800 N. Quincy St. Arlington, Va. 22217-5000</b>	
8a. NAME OF FUNDING/SPONSORING ORGANIZATION <b>SDI-ISTO</b>	8b. OFFICE SYMBOL (If applicable)	9. PROCUREMENT INSTRUMENT IDENTIFICATION NUMBER <b>N 00014-87-J-1258</b>	
8c. ADDRESS (City, State, and ZIP Code) <b>Washington DC 20301-7100</b>		10. SOURCE OF FUNDING NUMBERS	
		PROGRAM ELEMENT NO.	PROJECT NO.
		TASK NO.	WORK UNIT ACCESSION NO.
11. TITLE (Include Security Classification) <b>Novel Pulsed Plasma Treatment &amp; Coating Process: Multilayer Structures for Optical Computing Applications. Final Report.</b>			
12. PERSONAL AUTHOR(S) <b>I. P. Llewellyn &amp; R. A. Heinecke</b>			
13a. TYPE OF REPORT <b>Technical</b>	13b. TIME COVERED <b>FROM Aug. 88 TO Dec. 89</b>	14. DATE OF REPORT (Year, Month, Day) <b>1990/3/15</b>	15. PAGE COUNT <b>28</b>
16. SUPPLEMENTARY NOTATION			
17. COSATI CODES		18. SUBJECT TERMS (Continue on reverse if necessary and identify by block number)	
FIELD	GROUP	SUB-GROUP	
		Multiquantum wells, layer structures, non-linear optical materials, chalcogenide thin films, optical computing, optical filters, pulsed plasma germanium sulphide. (6)	
19. ABSTRACT The objective of this work has been to develop the technique and equipment required to use the STL pulsed plasma deposition process to produce amorphous multi-quantum well layered materials with layer thicknesses down to a few atoms. Such structures have many possible uses in defence-related areas, but at the request of SDI, work has concentrated on the use of the technique to produce non-linear optical materials with high third-order susceptibility for use in optical computing devices. In particular, we have shown that films based on thin layers of chalcogenide glasses show large non-linear effects of similar magnitude to those seen in optical filters, and have demonstrated that it may be possible to construct very fast optical devices (<250 ps) using this technique. Furthermore, this technology should be readily integrated with passive optical components such as optical filters in order to produce all the necessary elements for a parallel computing system. <i>Keywords:</i>			
20. DISTRIBUTION/AVAILABILITY OF ABSTRACT <input type="checkbox"/> UNCLASSIFIED/UNLIMITED <input type="checkbox"/> SAME AS RPT. <input type="checkbox"/> DTIC USERS		21. ABSTRACT SECURITY CLASSIFICATION <b>Unclassified/Unlimited</b>	
22a. NAME OF RESPONSIBLE INDIVIDUAL <b>Dr. R. Pohanka/Dr. W. Smith</b>		22b. TELEPHONE (Include Area Code)	22c. OFFICE SYMBOL

DD FORM 1473, 84 MAR

83 APR edition may be used until exhausted.  
All other editions are obsolete.

SECURITY CLASSIFICATION OF THIS PAGE

Distribution List

Dr. R. Pohanka	ONR, Arlington
Dr. W. A. Smith	ONR, Arlington
Dr. D. Dustin	SDI-ISTO, Washington
Dr. W. Miceli	ONR, Boston
Dr. F. Quelle Jnr.	ONR, Boston
Dr. H. E. Brandt	Harry Diamond Laboratories
Dr. K. Davis	ONR, Arlington
Mr. N. M. Yoder	ONR, Arlington
Dr. F. Bartoli	Naval Research Lab., Washington
Dr. A. Goodman	ONR, Arlington
Dr. M. Stroschio	Army Research Office
Dr. G. K. Waggoner	AFWAL, WPAFB, Dayton
Dr. G. F. Schmitt Jnr.	AFWAL, WPAFB, Dayton
Mr. K. Carnahan	Carnahan Associates
Dr. G. Chantry	SDIPO, London
Dr. K. Lewis	RSRE, Malvern
Dr. J. Savage	RSRE, Malvern
Mr. S. Warren	STC Components
Dr. I. G. Talmy	Naval Surface Weapons Center
Defense Documentation Center	
Defense Metals & Ceramic Info.	
Dr. R. W. Schwartz	Naval Weapons Center
B. Wilcox	Materials Sci. Office
Metal & Ceramics Prg.	Army Research Office
Elec. & Mats. Sci. Dir.	Air Force Off. of Sci. Res/NE
Dr. S. Block	National Bureau of Standards
Dr. M. A. Cappelli	Stanford University, Stanford
Dr. B. Dunn	University of California, Los Angeles
Dr. G. Geoffroy	Pennsylvania State University
Dr. A. Harker	Rockwell Int'l Science Center
Mr. R. A. Heinecke	STC Technology Ltd
Dr. L. C. Klein	Rutgers University
Dr. G. Messing	Pennsylvania State University
Dr. P. E. D. Morgan	Rockwell Int'l Sci. Center
Dr. R. Roy	Pennsylvania State University
Dr. S. Musikant	General Electric Co. Philadelphia

Accession For	
NTIS CRA&I	<input checked="" type="checkbox"/>
DTIC TAB	<input type="checkbox"/>
Unannounced	<input type="checkbox"/>
Justification	
By _____	
Distribution / _____	
Availability Codes	
Dist	Avail and/or Special
A-1	



## CONTENTS

	PAGE
LIST OF FIGURES	
SUMMARY	
1. INTRODUCTION	1
2. EXPERIMENTAL TECHNIQUES	2
2.1 Pulsed Plasma Deposition	2
2.2 Deposition Conditions	4
2.3 Analysis of Films	5
3. PROPERTIES OF FILMS	5
3.1 Basic Materials	5
3.2 Layer Structures	6
4. OPTICAL PROPERTIES	7
4.1 Absorption Spectra	7
4.2 Photoluminescence Spectra	8
4.3 Non-Linear Optical Behaviour	9
4.4 Integrated Optical Structures	11
5. CONCLUSIONS	11
6. ACKNOWLEDGEMENTS	12
7. PUBLICATIONS	12
REFERENCES	13

## LIST OF FIGURES

- Fig. 1 Schematic of the Pulsed Plasma Equipment
- Fig. 2 Variation of the 90% absorption point with ratio of the deposition gases for  $\text{GeS}_x$  and  $\text{GeSe}_x$
- Fig. 3 Auger depth profile of a 100 Å  $\text{GeS}_x:\text{SiO}_2$  multilayer stack
- Fig. 4 Infra-red absorption spectra of a. 3000 Å  $\text{SiO}_2$ , b. 1000 Å  $\text{GeO}_2$ , c. 80 layers in total of 50 Å alternate layers of  $\text{SiO}_2$  and  $\text{GeS}_x$ , d. 160 layers in total of 25 Å alternate layers of  $\text{SiO}_2$  and  $\text{GeS}_x$
- Fig. 5 Variation of the absorption edge,  $W$ , with layer thickness,  $L$ , for the  $\text{GeS}_x:\text{SiO}_2$  multilayer stacks
- Fig. 6 Variation of the conduction band energy with layer thickness using the Kronig-Penney model with  $m = 0.02$
- Fig. 7 Photoluminescence spectrum of 2000 Å of  $\text{GeS}_x$  and 51 layers in total of 50 Å alternate layers of  $\text{SiO}_2$  and  $\text{GeS}_x$
- Fig. 8 Transmission of 488 nm argon ion laser beam through 2000 Å of  $\text{GeS}_x$

CONTRACT NO. 00014-87-J-1258

August 1987 - December 1989

NOVEL PULSED PLASMA TREATMENT AND COATING PROCESS:  
MULTILAYER STRUCTURES FOR OPTICAL COMPUTING APPLICATIONS  
Final Report

SUMMARY

The objective of this work has been to develop the technique and equipment required to use the STL pulsed plasma deposition process to produce amorphous multi-quantum well layered materials with layer thicknesses down to a few atoms. Such structures have many possible uses in defence-related areas, but at the request of SDI, work has concentrated on the use of the technique to produce non-linear optical materials with high third-order susceptibility for use in optical computing devices. In particular, we have shown that films based on thin layers of chalcogenide glasses show large non-linear effects of similar magnitude to those seen in optical filters, and have demonstrated that it may be possible to construct very fast optical devices (<250 ps) using this technique. Furthermore, this technology should be readily integrated with passive optical components such as optical filters in order to produce all the necessary elements for a parallel computing system.

## 1. INTRODUCTION

The STL developed pulsed plasma deposition method is unique in its ability to deposit high quality films at or close to room temperature<sup>1,2</sup>. The method uses very high powered pulsed radio frequency (RF) discharges of gaseous precursors in order to dissociate the precursors to atomic species, which then re-combine at the surface of the substrate to form a film. The high power of the discharge causes complete dissociation of the precursors such that no further heating is required for completing the surface reactions as is found for conventional, low power, RF dissociation. The low duty cycle of the pulse keeps the RF average power low and hence the heating of the substrate is minimised. Furthermore, the relatively long time between RF pulses allows the type of precursor to be changed between pulses, and allows alternate layers to be deposited on an atomic scale.

In this work, the capability of the process to deposit layered structures has been fully explored and developed, with particular emphasis being placed on the production and evaluation of amorphous quantum wells of chalcogenide glasses as non-linear optical materials. These materials are thought to be good candidates for optical materials due to the observation of fast third-order non-linear behaviour in microcrystallites embedded in glass<sup>3,4</sup>.

The scope of this work was severely affected by cutbacks at SDI which resulted in only a small level of funding in 1989. Consequently, it was not possible to optimise the work in terms of material systems or composition, and hence the full capability of the deposited materials in the field of non-linear optics has not been evaluated. Nevertheless, the programme has been very successful in its objectives and has achieved many notable advances, as follows:

- The ability of the high-powered pulsed plasma facility at STL to produce amorphous multi-quantum well (MQW) structures down to less than 25 Å in thickness has been demonstrated.

- Films of chalcogenide glasses have been deposited, and shown to have similar properties to material prepared using conventional methods.
- Chalcogenide glass of structures  $\text{GeS}_x$  and  $\text{GeSe}_x$  have been deposited and have been shown to exhibit shifts of the band gap in agreement with quantum mechanical calculations.
- In conjunction with the University of Dublin, the deposited MQW films have been shown to have large non-linear optical coefficients, together with a very fast response (<250 ps).
- The band gap (and hence wavelength of greatest non-linearity) of the material can be altered by varying the composition of the film by changing the concentration of the atoms in the gas phase.
- The technique has been used to deposit etalons consisting of MQW materials between dielectric filter stacks. Further work is required to develop an optimised material with a higher non-linearity to absorption ratio, which would enable integrated structures of the kind required for optical computing to be formed in the one process.

## 2. EXPERIMENTAL TECHNIQUES

### 2.1 Pulsed Plasma Deposition

The pulsed plasma technique developed at STL is unique in that it can produce high quality films without requiring additional forms of heating of the substrate. With the deposition occurring at about room temperature, one of the main problems in making chalcogenide layer structures, namely the tendency of the materials to disproportionate at temperatures >500 K, is overcome. The equipment has been fully described in publications<sup>1,2</sup>. In this section we review how the technique works and how it has had to be adapted in order to produce sharp interface multilayer stacks.

The patented pulsed plasma technique relies on a very high power, short duration, discharge pulse completely dissociating a low pressure (0.1 mbar) gas into its constituent atoms. The atoms then diffuse to the substrate and other surfaces in the discharge chamber and condense to form the film. The pulse repetition rate is adjusted to give a low average power consistent with a low temperature process, and to allow the exchange of gases in the discharge chamber between pulses. Typical conditions are 50 kW RF power, 200  $\mu$ s pulsewidth, and a pulse repetition rate of 25 Hz. The method is differentiated from normal plasma deposition techniques in that very much higher RF powers are used, leading to much higher dissociation in the gas phase, so that substrate heating is no longer required to promote the surface reactions normally necessary in order to densify the film.

The apparatus is shown schematically in Figure 1. The chamber consists of a 150 mm diameter ISO six-way vacuum cross which is evacuated by a roots/rotary vacuum combination at a rate of 250  $\text{m}^3\text{h}^{-1}$ . Gas is passed into the chamber by a series of eight valves ( $SV_n$ ), mass flow controllers ( $MFC_n$ ), and fast solenoid valves ( $PV_n$ ). The conduction of the pipework is kept high so as to allow rapid change of gases in the chamber by operating the solenoid valves. Typically the gas can be changed between RF pulses, so as to allow change of deposited material in as little as 25 ms. The gas storage volumes ( $VOL_n$ ) are pressurised when the solenoid valves are closed in order to provide a reservoir of gas with which to fill the chamber to the desired operating pressure when the solenoid valves are opened. The discharge power is supplied from a high power 13.56 MHz RF generator which is coupled to the discharge via a standard 'L' type matching network. A microcomputer is used to control the gas handling, vacuum system, and RF pulsing. The substrate was placed onto the RF driven electrode.

Initially, flat electrodes were used in the chamber, but it was found impossible to produce sharp interfaces using this configuration due to the high self-induced d.c. bias that develops on the substrate leading to extensive sputtering of material at the film interfaces. Typical average bias levels during the pulse were 3000 V at 50 kW RF power levels. A large amount of effort was directed to reducing this bias, and the 'cup'

electrode configuration shown in Figure 1 was designed and built, which allowed the bias to be reduced to less than 100 V at 50 kW RF discharge power. The precise mechanism for this effect is unclear; the change in electrode area between the flat and cup electrode is not large enough alone to explain this very large reduction.

The change in impedance of the discharge as the gas is varied in the chamber is large enough to require large changes in the value of the variable capacitors in the matching network in order to maintain maximum power transfer from the generator to the discharge. However, when depositing layered structures, it is not possible to alter the matching capacitors between depositing different layers, and, for this work, a new method was employed. Argon was added to the depositing gas in sufficiently large quantities to dominate the impedance of the discharge so that a mean matching point could be used for both layers. Generally 80% of the chamber pressure was argon, but this appeared to have no effect on the properties of the films. Using this technique, the time required to change over between depositing one layer and another was very rapid, being typically 20 ms. This, coupled with the very high rates of deposition that are obtained in the pulsed plasma technique, up to 0.3  $\mu\text{m}$  per minute, enabled a large number of layers to be deposited in just a few minutes.

## 2.2 Deposition Conditions

Films of silicon dioxide were produced using the precursors silane and carbon dioxide. Typical conditions were 50 sccm of silane mixed with 200 sccm of carbon dioxide and 800 sccm of argon, with a pulsewidth of 150  $\mu\text{s}$  and a pulse repetition rate of 25 Hz. The films were of high quality, and exhibited negligibly low concentrations of hydrogen when analysed using Fourier transform infra-red spectrometry. The properties of these films have been published<sup>1</sup>.

Films of germanium sulphide or germanium selenide were produced from germane and hydrogen sulphide or hydrogen selenide as starting materials respectively. Typical flows were 50 sccm of germane and 20 to 200 sccm of the chalcogenide source with 800 sccm of argon. Varying the ratio of the flow of the depositing gases allows the composition of the

films to be varied. The RF pulsewidth was 200  $\mu$ s with a pulse repetition rate of 25 Hz. Typical deposition rates were about 600  $\text{\AA}$ /minute.

### 2.3 Analysis of Films

Absorption spectroscopy of the deposited films was performed both in the visible/ultra-violet region and in the infra-red region. For the visible/ultra-violet spectra the films were deposited onto glass slides and for the infra-red spectra the films were deposited on germanium substrates. A Fourier transform spectrometer was used to take the infra-red spectra, which allowed the background spectra of the germanium to be subtracted, leaving the spectra of the film alone. Since the films were thin, spectra taken at normal incidence gave large interference peaks. A new method has been devised to eliminate these peaks by using plane polarised light and the sample placed at Brewster's angle in order to obtain good spectra. Great care was taken in getting the correct angle to completely remove the fringes and in some spectra small fringes remained.

Auger and scanning electron microscopy (SEM) examination were performed on films deposited onto (100) silicon wafers. The layered films were profiled by alternately ion beam milling of the surface and Auger analysis. Two ion guns incident on the sample at 55 degrees to the normal were used in order to obtain uniform etching. The etching used argon ions accelerated to 750 V at a total current density of 2  $\mu\text{A cm}^{-2}$  which gave an etching rate of about 1  $\text{\AA}$ /minute. SEM examination was performed in equipment that was also equipped for x-ray microanalysis, allowing the composition of films to be determined.

## 3. PROPERTIES OF FILMS

### 3.1 Basic Materials

The versatility of the pulsed plasma technique means that a much wider range of material stoichiometry can be made than is possible with more conventional techniques. For example, germanium sulphide can be made in a wide range of compositions with band gaps ranging from 350 nm in the ultra-violet to 750 nm in the infra-red. Germanium selenide gave

similar results, but the band gap can only be shifted over a more limited range, from 460 nm to 650 nm. Figure 2 shows the variation of the band edge of  $\text{GeS}_x$  and  $\text{GeSe}_x$ , as determined from the absorption spectra, as a function of the ratio of germane to hydrogen sulphide or hydrogen selenide. Films with a ratio of selenium to germanium greater than five appear to have no band edge absorption, have a metallic lustre, and are photoconductive.

Good correlation was found between the film composition expected from the gas flows to that obtained using microanalysis. For example when the ratio of  $\text{GeH}_4:\text{H}_2\text{Se}$  was 1:4, the microanalysis gave a Ge:Se ratio of 1:3.9. When  $\text{GeH}_4:\text{H}_2\text{Se}$  was 2:1, the microanalysis gave a Ge:Se ratio of 1.8:1, both of which agree to a satisfactory level considering the difficulty of correcting for x-ray self-absorption in the films.

### 3.2 Layer Structures

Figure 3 shows a typical Auger depth profile of a germanium sulphide/silicon oxide multilayer stack. The alternate layers can be clearly seen over several orders in the silicon, oxygen, germanium and sulphur Auger signals. The profile shows an apparent loss of resolution with depth due to the ion beam sputtering not being completely uniform over the analysis area. For very thin layers (<50 Å) this effect limits the usefulness of the technique to profiling the first couple of layers.

The resolution of the depth profile depends both on the escape depth of the Auger electron and the degree to which the ion sputtering roughens the surface. The former depends on the energy of the Auger electron and the nature of the surface, and the resolution was optimised in this work by the use of the lowest energy signals for the elements whenever possible. The effect of the ion sputtering was minimised by using a very low sputtering rate, but even with these precautions it was clear that the profile of the interface between the layers was mainly due to the limited resolution, and only limited information could be obtained about the nature of the interface between the layers using this technique alone.

However, detailed chemical information about the interface can be obtained using infra-red absorption spectroscopy. This was particularly easy to carry out since both pulsed plasma deposited germanium sulphide and germanium selenide have no major peaks in the infra-red. Hence the germanium chalcogenide/silicon dioxide stacks should have spectra which show only peaks associated with silicon-oxygen bonds and those associated with the bonds formed at the interface (for example Ge-O, S-O bonds). Figure 4 shows the infra-red spectra of pulsed plasma deposited  $\text{GeS}_x/\text{SiO}_2$  multilayer stacks together with the spectra of pulsed plasma deposited silicon oxide and germanium oxide (made from a discharge of  $\text{GeH}_4$  and  $\text{CO}_2$ ) for comparison. The spectra agree well with those published<sup>5</sup> for silicon oxide and germanium oxide, which assign the band at  $1065\text{ cm}^{-1}$  to Si-O stretching, the band at  $820\text{ cm}^{-1}$  to Si-O bending and the band at  $860\text{ cm}^{-1}$  to Ge-O stretching. The layered structures show both Si-O bands clearly, but fail to show any Ge-O peaks even for a layer as thin as 25 Å. This suggests that the interface occurs abruptly and there is little or no interface 'smearing' between the layers. It should be noted that it is not possible to monitor accurately the formation of S-O bonds at the interface using this technique, since the S-O bands at  $1060\text{ cm}^{-1}$  overlap the Si-O stretching bands. However, the constant ratio of the Si-O stretching band to the intensity of the Si-O bending band in the spectra of the silicon oxide and the layered structures seems to imply that the number of S-O bonds present in the multilayers is small. There is also no sign of increased hydrogen bond inclusion at the interface as has been found in plasma deposited a-Si:H/a-SiN<sub>x</sub>:H multilayer structures<sup>6</sup>.

#### 4. OPTICAL PROPERTIES

##### 4.1 Absorption spectra

The absorption edge of both the  $\text{GeS}_x/\text{SiO}_2$  and  $\text{GeSe}_x/\text{SiO}_2$  multilayer stacks shifts to the blue as the chalcogenide layer thickness decreases, in a similar manner to the shift seen in chalcogenide microcrystalline colloid filters as the particle size gets smaller<sup>3</sup>. Figure 5 shows the variation of the band edge found using the 90% absorption point as the layer thickness decreases in a  $\text{GeS}_x/\text{SiO}_2$  multilayer.

The shift is thought to result from the quantum confinement of the electron within the layer and is modelled theoretically by a three dimensional electron gas in a one dimensional periodic square-wave potential, the Kronig-Penney model<sup>7</sup>. This states that the shift in the position of a band on confinement is given by:

$$1 = \frac{A^2 - B^2}{2AB} \sinh(AL_A) \sin(BL_B) + \cosh(AL_A) \cos(BL_B) \quad (1)$$

where  $A^2 = \frac{8\pi^2 m(U-E)}{h^2}$  and  $B^2 = \frac{8\pi^2 m E}{h^2}$  (2)

In this equation  $m$  is the effective mass of the electron,  $h$  is Planck's constant,  $L_A$ ,  $L_B$  are the layer thicknesses, and  $U$  is the potential energy barrier. The band gap shift is the difference in the shift of the valence band and the shift in the conduction band. However, since the valence bands for  $\text{GeS}_x$  and  $\text{SiO}_2$  are probably quite close in energy, we assume here that the shift is caused only by the shift in the conduction band in the  $\text{GeS}_x$ . The above equations were solved on a digital computer for the  $\text{GeS}_x/\text{SiO}_2$  layered structures using a band gap in the  $\text{SiO}_2$  of 6.2 eV (based on the observed onset of absorption in the material at 200 nm), and a band gap in  $\text{GeS}_x$  of 2.48 eV (corresponding to an absorption band edge of 500 nm). The effective mass was treated as a variable parameter which could be altered to adjust the model to fit the data. The fit with the smallest sum of squares of the deviations from the data has  $m = 0.01 m_0$  and is shown in Figure 6. Although no data exists for the conduction band effective electron mass in these materials, this figure is of the same order of magnitude as is found in many compound semiconductor materials<sup>8</sup>.

#### 4.2 Photoluminescence spectra

Photoluminescence spectra of the  $\text{GeS}_x$  material and  $\text{GeS}_x/\text{SiO}_x$  multilayer structures were obtained using argon ion laser excitation at liquid helium temperatures, and are shown in Figure 7. The spectra show photoluminescence over a large wavelength range, but which peaked in the near infra-red. The spectra are similar to those obtained from

chalcogenide glasses produced from other means<sup>8</sup>. The large Stokes' shift seen in such materials is thought to be caused by defect states in the band gap. It is interesting to note that the radiation from these defect states is also blue-shifted in the layered structure; for the 50 Å layers shown in Figure 7 the shift is 33 nm from that of the bulk material.

#### 4.3 Non-Linear Optical Behaviour

When excited near their band edge, chalcogenide-containing glasses have been shown to have large third-order susceptibilities and consequently experience large changes in their refractive index and absorption coefficients under laser irradiation<sup>3,8</sup>. In this section we present preliminary results on the optical behaviour of  $\text{GeS}_x$  and  $\text{GeS}_x:\text{SiO}_2$  multilayer stacks.

In order to search for changes in the absorption coefficient or refractive index of the films under high photon fluxes, the deposited films were irradiated with a high intensity laser beam from an argon ion laser. Since the laser wavelength could not be tuned continuously, it was necessary to tailor the band gap of the film relative to that of the laser wavelength, and by varying the Ge:S ratio and layer size, samples were made that had band gaps corresponding to the energy of the 488 nm argon ion line. These samples were then placed in the laser beam at 45 degrees and the incident, reflected, and transmitted light powers were recorded as the beam energy was varied. No beam focusing was used and the diameter of the approximately Gaussian beam was estimated to be 2 mm. Up to 2 W of laser power could be used before the sample showed signs of irradiation induced damage.

For both the bulk GeS material and the layered structure there was always a linear dependence of reflected and incident laser power, indicating that no major change in the refractive index occurs on irradiation. This test is a very crude measure of refractive index; by computer modelling<sup>9</sup> of the change in reflectance with refractive index we would not have expected a change in index of less than 0.05 to be detectable.

The transmitted light through the films showed a large non-linear variation with laser power, with an increase in the absorption coefficient with increased laser power. Figure 8 shows the transmitted laser beam intensity through a 2000 Å  $\text{GeS}_x$  film as the incident power is varied. All the films, both layered or not, that had part of their band tail at the laser wavelength showed some non-linearity, whereas those films which had band gaps away from the laser wavelength did not. The non-linearity was entirely reproducible on repeating the experiment thus demonstrating that the effect was not caused by laser damage. However, irradiation using a continuous laser causes a temperature rise in the film, and it is difficult to ascertain whether the induced absorption is a thermal effect, an electronic effect, or a mixture of both.

In order to investigate the non-linear behaviour of the films in more detail, measurements were made on the third-order susceptibility near the band edge using the degenerate four-wave mixing technique described in reference 10 and a nitrogen-pumped dye laser as the source. The results show that the third-order susceptibility is proportional to the absorption coefficient at that wavelength. For an absorption of  $2.8 \times 10^4 \text{ cm}^{-1}$ , the bulk material has a third-order susceptibility of  $4 \times 10^{-8}$  e.s.u., a value which is comparable with that observed for chalcogenide based filters. With layering, the effect is considerably enhanced; such that for a 50 Å thick  $\text{GeS}_x:\text{SiO}_2$  layer structure, the susceptibility for a given absorption is increased by a factor of five. The optical response is also fast, since it can be measured with the nitrogen-pumped dye laser system (pulsewidth 250 ps). Consequently, it is unlikely that the effect is thermal in origin but is more likely to be directly related to a redistribution of electron populations following photon excitation. The effect also increases as the band gap is approached. Table 1 shows this for values of the third-order susceptibility for a 5 nm MQW device. It should be noted that due to the increase in absorption near the band gap, it will probably not be worthwhile to make a bistable device close to the band gap, and further detailed studies will be required to work out the optimum non-linearity/absorption ratio.

#### 4.4 Integrated Optical Structures

One of the prime objectives of this work was to demonstrate that the pulsed plasma process can be used to produce integrated optical devices by making etalons, where a non-linear material is used as a spacer between two passive reflection stacks. In this way, optical non-linearity could be enhanced and optical bistable arrays could be produced.

In order to test the feasibility of this approach, the pulsed plasma technique has been developed to allow the deposition of dielectric thin film reflection filters. In particular, filters have been deposited using silicon dioxide ( $n$  of 1.45) and silicon nitride ( $n$  of 2.0) at room temperature. Furthermore, no active thickness measurement technique needs to be used, since the thicknesses of the deposited films can be accurately predicted simply by counting pulses. In this way, etalon stacks of MQW devices have been produced but a much more detailed study will be required in order to evaluate and optimise them.

#### 5. CONCLUSIONS

The work carried out during the contract period has demonstrated the first successful attempt at depositing at room temperature high quality, essentially hydrogen free, layered structures of the chalcogenide semiconductors  $\text{GeS}_x$  and  $\text{GeSe}_x$ , and  $\text{SiO}_2$ . Results are presented that suggest that these films could have useful optical properties in the production of both passive optical filters and active optical devices. In particular, the comparatively low laser power density that is required to observe a non-linear optical response in these materials ( $<10 \text{ kWcm}^{-2}$ ), the fast response of the effect ( $<250 \text{ ps}$ ), and the ability to select the band gap, could make these materials important in the production of all-optical logic gates, compatible with available solid state laser sources.

The work appears promising as a candidate for an active optical technology, but further work needs to be performed on the mechanisms involved in order to optimise the effect. In particular, the effect will need to be studied as both a function of material and of composition. The program has concentrated on  $\text{GeS}_x$  and  $\text{GeSe}_x$  purely on the grounds of the

ready supply of high quality precursors, and it is interesting to note that the largest measurements of non-linearity in chalcogenide to date have been using microcrystalites of cadmium chalcogenides. It is also to be expected that the composition of the films should have an impact on the effect, and, by careful study, should enable an optimum effect to be obtained.

#### 6. ACKNOWLEDGEMENTS

The work has benefitted from inputs from Dr. Blau of the University of Dublin, on the evaluation of stacks by DFMT, and T. Clapp of STL, for suggesting the use of glassy chalcogenides.

#### 7. PUBLICATIONS

The following publications by STL have been supported in part or fully by this contract:

Low Temperature Pulsed Plasma Deposition. Part 1 - A New Technique for Thin Film Deposition with Complete Gas Dissociation, G. A. Scarsbrook, I. P. Llewellyn, S. M. Ojha and R. A. Heinecke, Vacuum 38(8-10), 627, 1988.

Low-Temperature Pulsed Plasma Deposition. II. The Production of Novel Amorphous Compounds of Germanium in Thin Film, G. Scarsbrook, I. P. Llewellyn and R. A. Heinecke, J. Vac. Sci. Technol. A 7(3), 1099, 1989.

Low Temperature Pulsed Plasma Deposition Part 3: A Method of Deposition of Aluminium and Tin At Room Temperature, I. P. Llewellyn, N. Rimmer, G. A. Scarsbrook, R. A. Heinecke, to be published in Thin Solid Films, 1990.

Low Temperature Pulsed Plasma Deposition: Part 4: The Preparation of Layered Structures of Amorphous Chalcogenide Glasses with Non-Linear Optical Properties, I. P. Llewellyn, G. A. Scarsbrook, R. A. Heinecke, presented at the SPIE's 33rd Annual International Symposium, San Diego, California, 1989.

## REFERENCES

1. G.A. Scarsbrook, I.P. Llewellyn, S.M. Ojha, R. Heinecke, *Vacuum* **38**(8-10), 627, 1988.
2. G.A. Scarsbrook, I.P. Llewellyn, R. A. Heinecke, *J. Vac. Sci. Technol. A* **7**(3), 1099, 1989.
3. H.P. Rooksby, *J. Soc. Glass Technol.* **16**, 171, 1975.
4. H.E. Eichler, G. Enterlein, P. Glozback, J. Munschau, H. Stahl, *Appl. Opt.* **11**, 372, 1972.
5. J.C. Rostaing, Y. Cros, S.C. Gujrathi, S. Poulain, *J. Non-Cryst. Solids*, **97**, 1051, 1987.
6. C.B. Roxlo, B. Abeles, P.D. Persans, *J. Vac. Sci. Technol. B* **4**(6), 1430, 1986.
7. C. Kittel, "Introduction to Solid State Physics", 5th ed. p.191, J. Wiley & Sons, N.Y., 1976.
8. K.C. Rustagi, C. Flytzanis, *Opt. Lett.* **9**(8), 344, 1984.
9. H.A. Macleod, "Thin Film Optical Filters", 2nd Edition, p.32, Adam Hilger, Bristol, 1986.
10. P. Horan, W. Blau, H. Byrne, P. Berylund, Submitted *Appl. Opt.* 1989.
11. C.B. Roxlo, B. Abeles, *Phys. Rev. B* **34**, 2522, 1986.
12. T. Tiedje, B. Abeles, P.D. Persans, B.G. Brooks, G.D. Cody, *J. Non-Cryst. Solids* **66**, 345, 1984.
13. H.T. Grahn, Z. Verdeny, H.J. Maris, J. Tauc, B. Abeles, *Mat. Res. Symp. Proc.* **77**, 265, 1987.

14. T. Hamasaki, J. Non-Cryst. Solids, 59, 679, 1983.
15. F. Henneberger, H. Rosman, Phys. Status Solidi b 121, 685, 1984.
16. B.S. Wherrett, S.D. Smith, F.A. Tooley, A.C. Walker, Future Generations Comput. Syst. 3, 253. 1987.

Wavelength/nm	Absorbance/cm <sup>-1</sup>	$\chi^3$ /e.s.u.
500	0.629	$3.11 \cdot 10^{-8}$
505	0.577	$4.07 \cdot 10^{-8}$
510	0.538	$2.94 \cdot 10^{-8}$
515	0.488	$2.06 \cdot 10^{-8}$
520	0.450	$1.60 \cdot 10^{-8}$
525	0.409	$1.53 \cdot 10^{-8}$
530	0.377	$1.27 \cdot 10^{-8}$
535	0.347	$1.08 \cdot 10^{-8}$
540	0.319	$1.95 \cdot 10^{-8}$

Table 1. Variation of the third-order susceptibility ( $\chi^3$ ) as a function of absorbance near the band edge for a 10 nm multiquantum well of GeS<sub>x</sub> and SiO<sub>2</sub>.

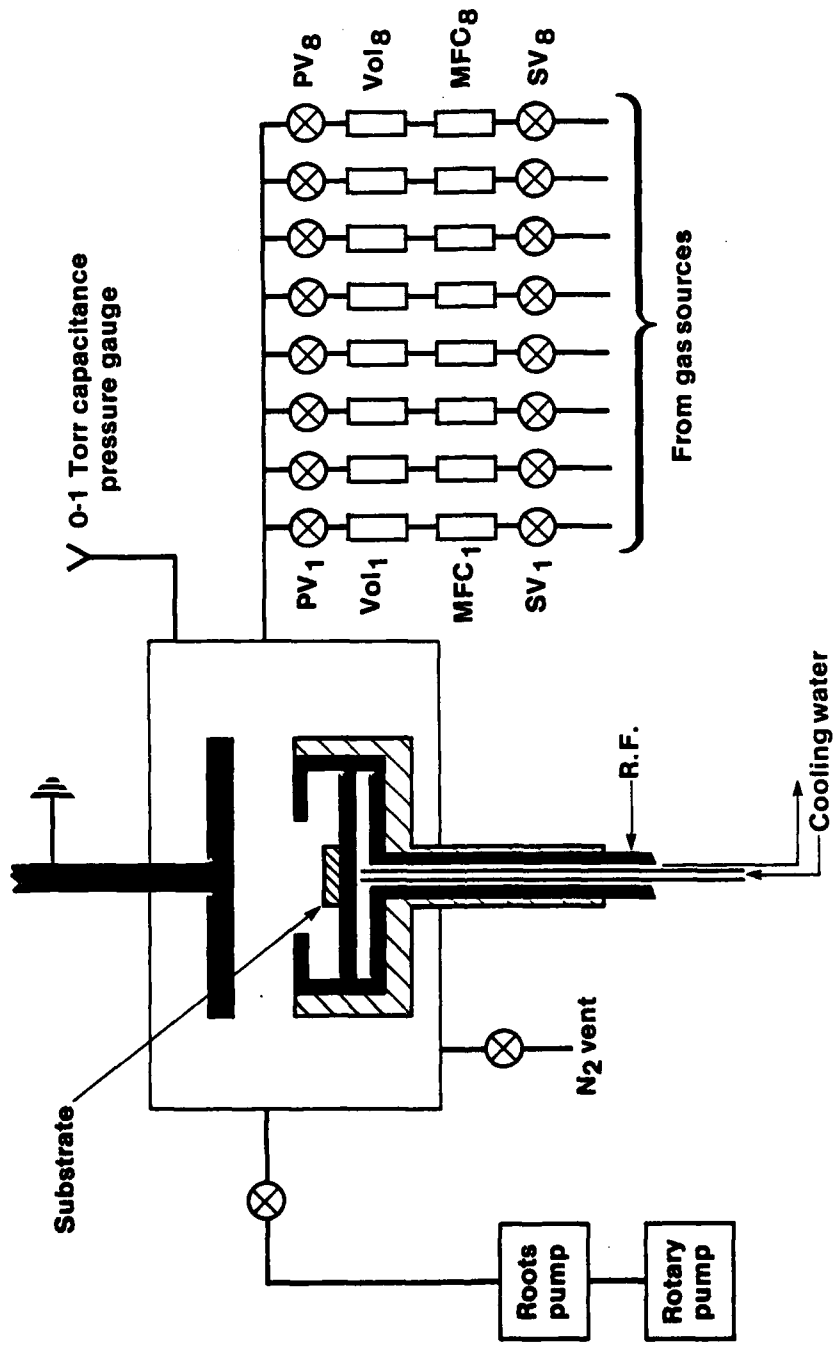


Fig. 1

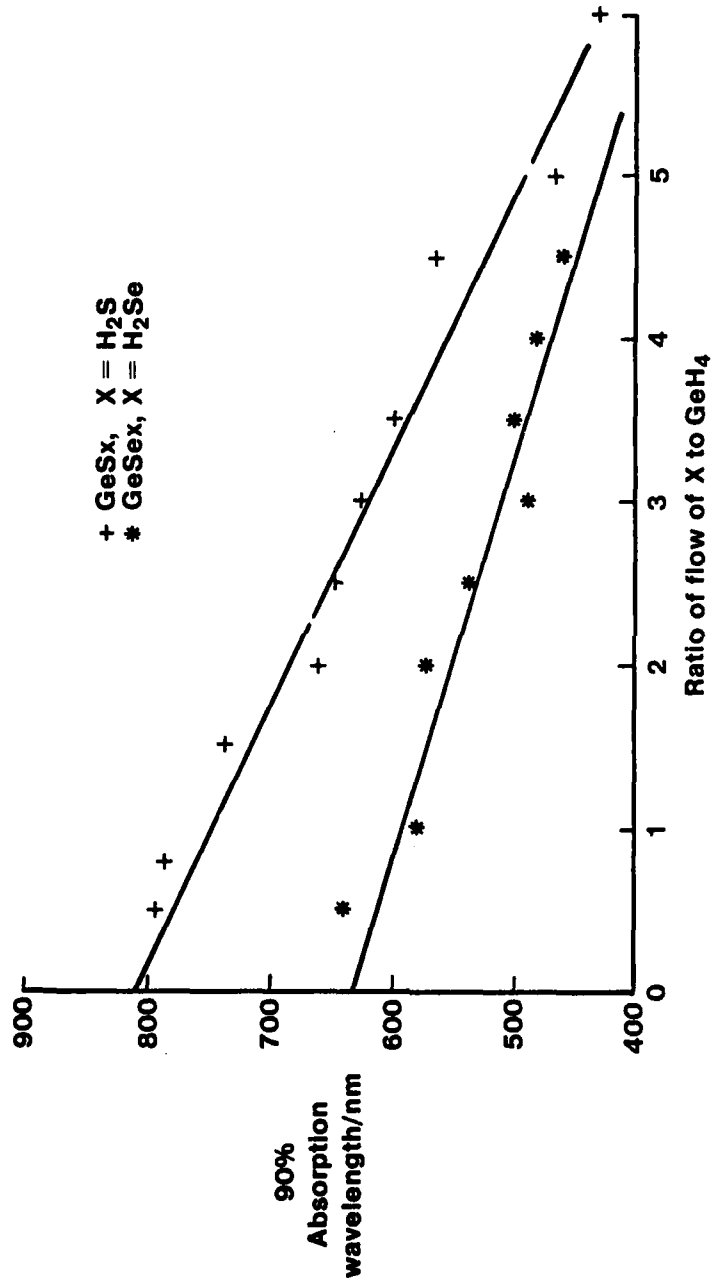


Fig. 2

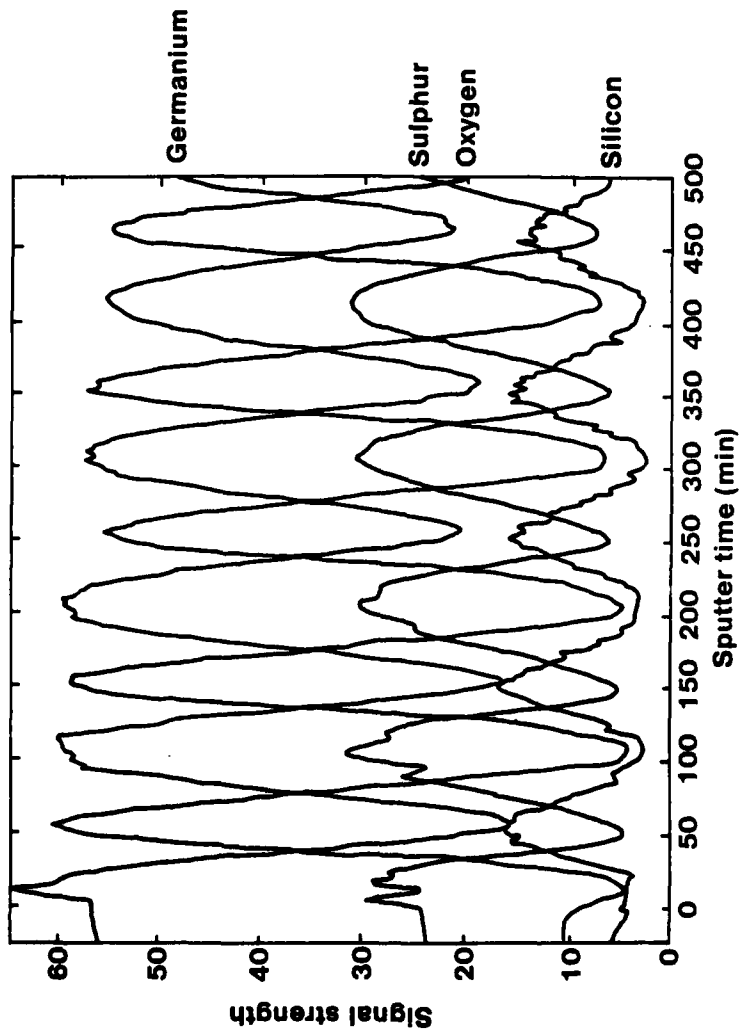


Fig. 3

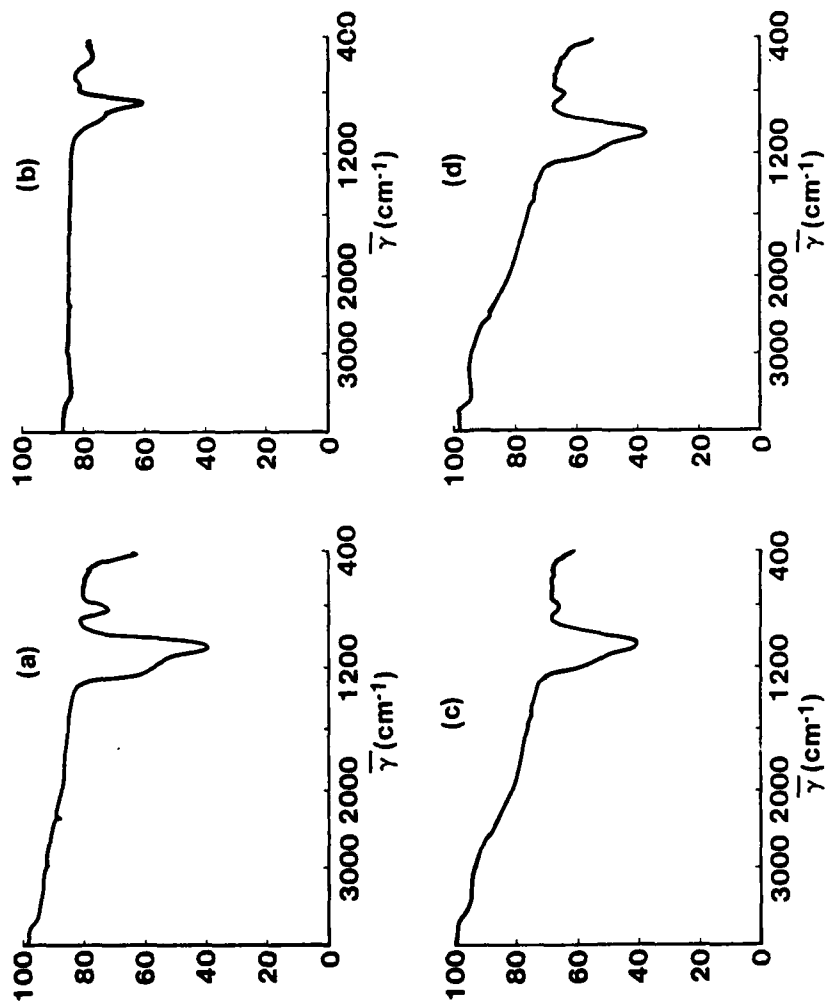


Fig. 4

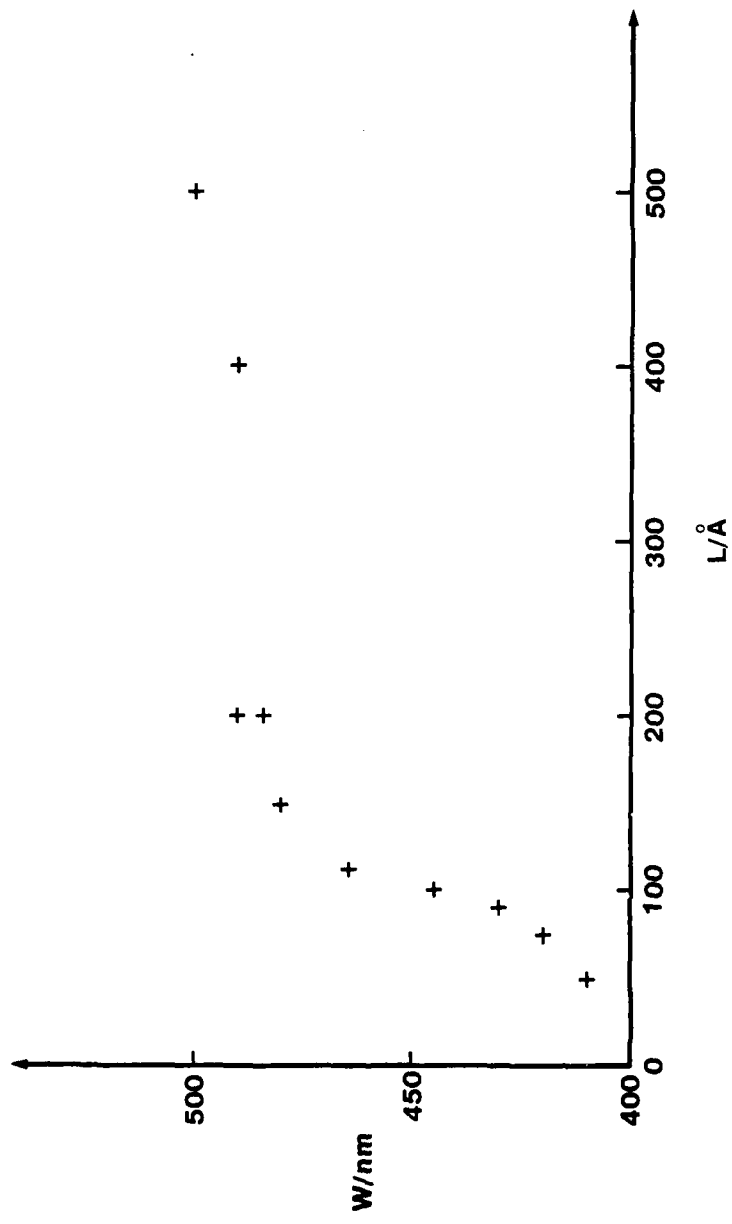


Fig. 5

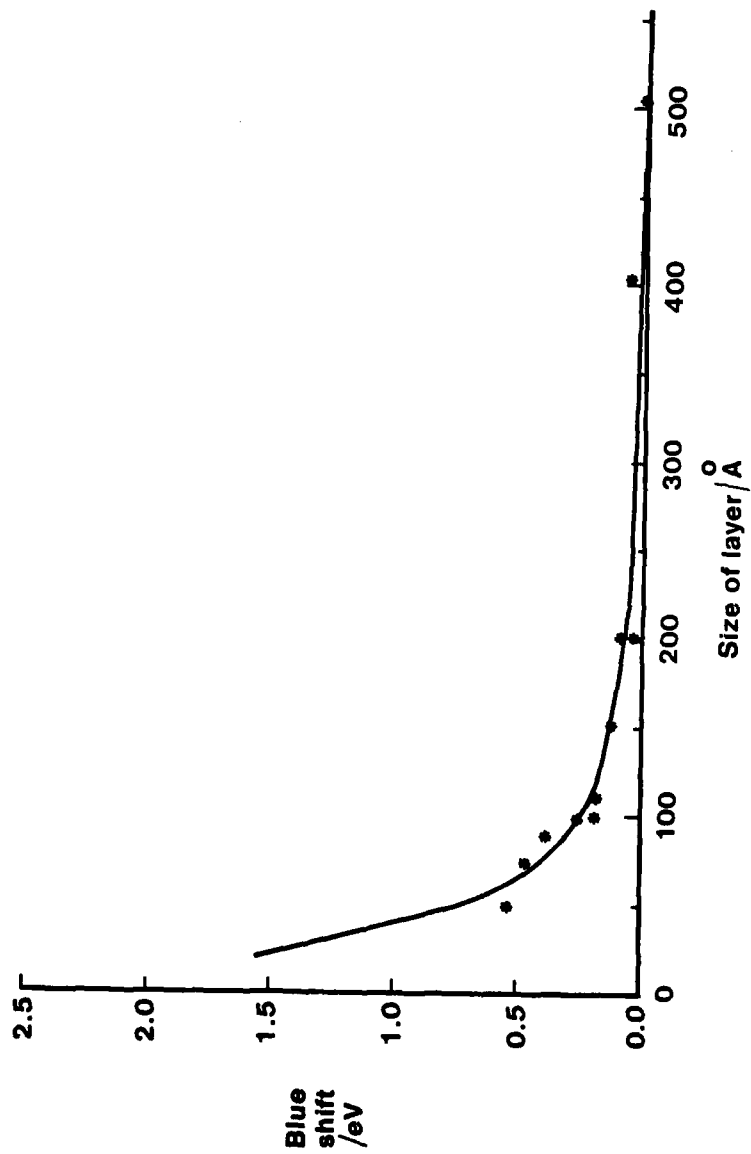


Fig. 6

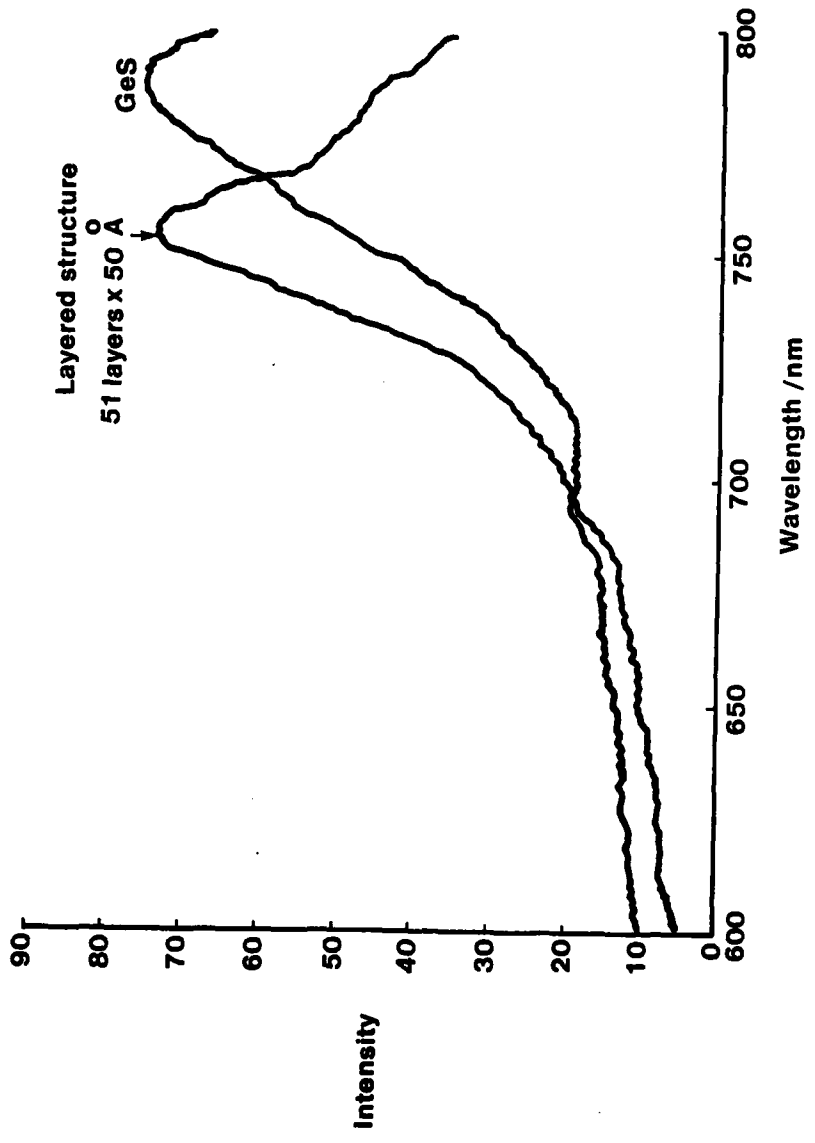


Fig. 7

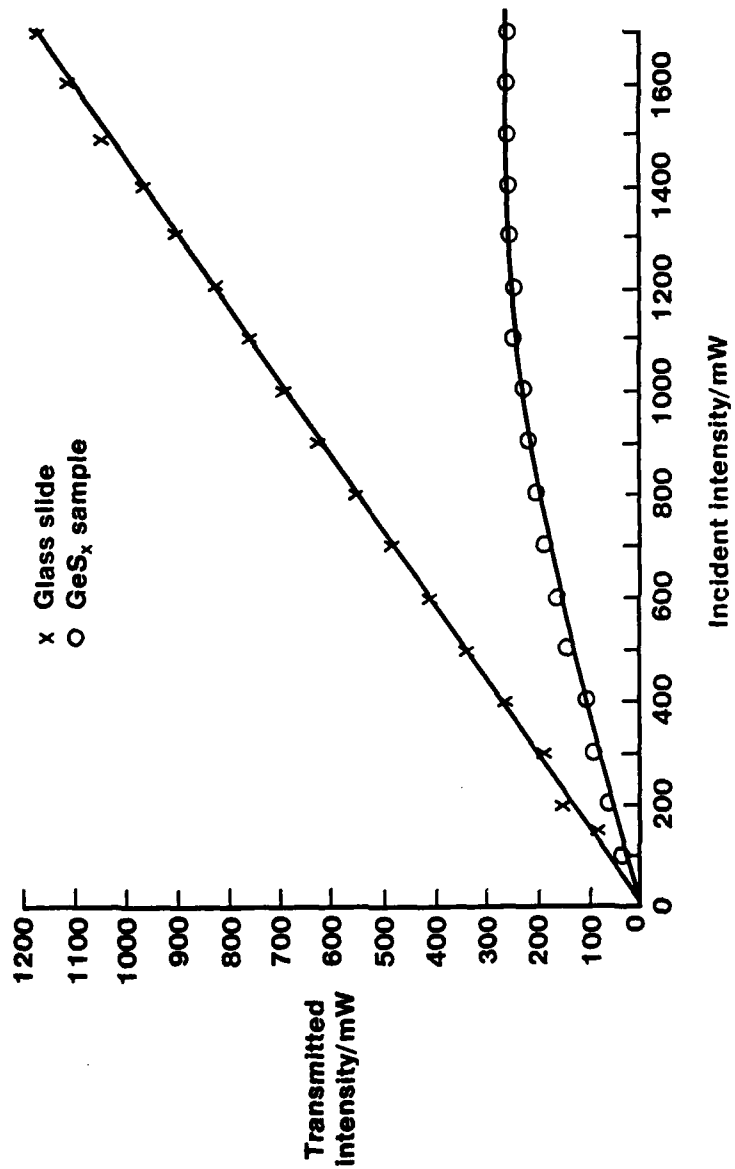


Fig. 8